

Current conservation and ratio rules in magnetic metals with Coulomb repulsion

Kosuke Odagiri

Electronics and Photonics Research Institute, National Institute of Advanced Industrial Science and Technology, Tsukuba Central 2, 1-1-1 Umezono, Tsukuba, Ibaraki 305-8568, Japan

December 2011

Abstract. From general considerations of spin-symmetry breaking associated with (anti-)ferromagnetism in metallic systems with Coulomb repulsion, we obtain interesting and simple all-order rules involving the ratios of the densities of states. These are exact for ferromagnetism under reasonable conditions, and nearly exact for anti-ferromagnetism. In the case of ferromagnetism, the comparison with the available experimental and theoretical numbers yields favourable results.

PACS. 11.40.-q Currents and their properties – 75.10.-b General theory and models of magnetic ordering

Contents

1	Introduction	1
2	The ferromagnetic ratio rule	2
3	Analysis of spin current conservation	6
4	Calculation of the parameters	10
5	Conclusions and Outlook	13

1 Introduction

1.1 Theoretical background

As is obvious and well known [1], magnetic order breaks $SU(2)$ spin symmetry (hereafter called $SU(2)_{\text{spin}}$). This gives rise to gapless excitations in the form of Nambu–Goldstone modes which are magnons and, according to the Goldstone theorem, excitations with energy gap, which may be called the Higgs bosons.

These excitations behave like elementary fields, and their interaction is central to spin-current conservation but, at the same time, they comprise of electrons with which they interact: i.e., they are composite. This imposes severe constraints on the properties of these fields, which we aim to discuss and exploit in this paper.

The same situation, of Goldstone fields (i.e., both Goldstone and Higgs fields) that are themselves composite objects, arises notably in two problems in the context of high-energy physics. The first problem is that of axial symmetry breaking at low energy scales due to the $SU(3)_C$ strong interaction. The Goldstone bosons here are pions. The second problem is that of electro-weak symmetry breaking. Although in the Standard Model, the Higgs field, or the doublet order-parameter field for $SU(2)_L \otimes U(1)_Y$, is an elementary scalar field, it is an attractive possibility that

this field is composite and, for example, is composed of quarks which bind strongly at high scales due to some interaction (N.B. not by the $SU(3)_C$ strong interaction which is weakly interacting at those scales). The low-energy phenomenology would then not be dissimilar to that of the Standard Model, but with some constraints on quantities such as the Higgs-boson mass.

A new approach to these problems, due to Gribov, have appeared in refs. [2,3,4,5]. These involve the idea of super-criticality and a self-consistent treatment of the fermion and Goldstone fields in the presence of the super-critical interaction. We shall make use of, and extend, the methods presented therein, to the case of magnetism. As for the other approaches to these old problems, see, for example, ref. [6] for an old approach to the first problem, and ref. [7] for an overview of the various methods and techniques developed to handle the second problem.

1.2 Outline of the paper

Our work concerns systems of electrons (or holes) which interact under a generalized Coulomb exchange (i.e., exchange of a generic gapless photon). We consider the system in the spin-symmetry-broken phase that arise in ferromagnetism and anti-ferromagnetism.

Our aim is to obtain exact relations between quantities that characterize the spin-symmetry-broken phase using the Dyson–Schwinger equations. This is possible because of the presence of the Ward–Takahashi identities which arise because of the conservation of spin symmetry. It turns out that the form of the Coulomb interaction does not affect these relations. The Coulomb interaction does affect, for instance, the electronic self-energy, but these are incorporated in the relations in a general way.

Before presenting the full analytical framework, we start with the simple case of the discussion of ground-state stability in ferromagnetism, in sec. 2. This gives rise to an exact rule for ferromagnetism which involves the electronic densities of states. We discuss this case with illustrations and a physical interpretation.

The full framework, which employ current-conservation techniques, is developed in secs. 3 and 4. In sec. 3, the interaction is worked out and presented in the form of Feynman rules. In sec. 4, the parameters of the interaction is worked out. This gives rise to an exact rule for anti-ferromagnetism which involves the electronic densities of states, but which involves the bare spin exchange energy.

The conclusions are stated at the end.

2 The ferromagnetic ratio rule

Before we introduce the full framework, let us discuss the stability of the ferromagnetic ground state as an illustrative example. We do so because this is a relatively simple problem, which does not require the full formalism, and which nevertheless leads to a strikingly simple and useful ratio rule. We shall expand the methods introduced here to build the formalism later.

2.1 Description of the system

Let us write the electrons in the $SU(2)_{\text{spin}}$ doublet form:

$$\psi_a \equiv \begin{pmatrix} \psi_\uparrow \\ \psi_\downarrow \end{pmatrix}. \quad (1)$$

The Lagrangian has the form:

$$\mathcal{L} = \delta_{ab} \psi_a^* \left(i \frac{\partial}{\partial t} - \epsilon(-i\nabla) - e\Gamma^\mu A_\mu \right) \psi_b + (\text{photon K.E.}) \quad (2)$$

A_μ is the electro-magnetic field, of which we shall retain only the electrostatic term A_0 later, as the contribution of the 3-vector potential is suppressed by the speed of light. The photon kinetic energy term may then be taken to be $-(\nabla A_0)^2/2$, which leads to an electrostatic $1/r$ interaction. ϵ refers to the dispersion relation of the electron. e is the electro-magnetic charge, which is defined to be negative for electrons. Γ^μ is the vertex function, whose time component is 1 for a Lagrangian of this form.

In the absence of magnetic order, the system is invariant under both the electromagnetic $U(1)_{\text{EM}}$ and the $SU(2)_{\text{spin}}$ rotations of ψ , where the latter is represented by

$$\mathcal{U}(\phi_i) \equiv \exp(i\sigma^i \phi_i/2). \quad (3)$$

σ^i ($i = 1, 2, 3$) are the Pauli matrices and ϕ_i are the rotation angles. Note that we are referring to global rotations here. Invariance under local rotations requires the presence of gauge fields such as the electromagnetic field, including the vector potential part and written in a gauge-invariant fashion.

There are two conserved currents, which are orthogonal. The first is the $U(1)_{\text{EM}}$ current:

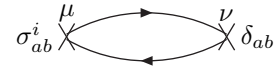
$$J_{\text{EM}}^\mu = \psi_a^* \delta_{ab} \Gamma^\mu \psi_b. \quad (4)$$

μ refers to the time-space four-vector index ($=0, 1, 2, 3$).

The second is the $SU(2)_{\text{spin}}$ current. This is written as

$$J_{\text{spin}}^{\mu,i} = \psi_a^* \sigma_{ab}^i \Gamma^\mu \psi_b. \quad (5)$$

Let us indicate the current diagrammatically by a cross. We see that current-current mixing, which we denote as $\Pi_{\text{mixing}}^{\mu\nu}$ and whose lowest order term is given by



$$\sigma_{ab}^i \text{---} \mu \text{---} \nu \text{---} \delta_{ab} \quad (6)$$

vanishes by symmetry for all i to all perturbative orders, and therefore the two currents are orthogonal.

When there is magnetic order, there arises, locally, a preferred orientation of spin, let us say along \downarrow , and this breaks the $SU(2)_{\text{spin}}$ symmetry, viz:

$$SU(2)_{\text{spin}} \longrightarrow U(1)_z. \quad (7)$$

As a result, there arises two Goldstone modes whose coupling is proportional to linear combinations of $\sigma^{1,2}$, and a Higgs mode whose coupling is proportional to σ^3 . The residual symmetry $U(1)_z$ refers to the symmetry under rotation by the generator σ^3 :

$$\mathcal{U}(\phi_3) \equiv \exp(i\sigma^3 \phi_3/2) \equiv \text{diag}(e^{i\phi_3/2}, e^{-i\phi_3/2}). \quad (8)$$

The form of the effective theory will be discussed later.

2.2 $U(1)$ current mixing

A result, which is almost trivial but possibly not previously discussed explicitly, is that after this symmetry breaking, the currents are no longer orthogonal. Equation (6) is easily calculated. Of particular interest is the $0-0$ component of eqn. (6) for $i = 3$ (i.e., the $U(1)_z$ current: $i = 1, 2$ vanish) at zero external energy and momenta. The vertex function Γ^0 being equal to 1 when the electrons are Fermi-liquid-like for each spin orientation, we obtain

$$\Pi_{\text{mix}}^{00} = \lim_{q \rightarrow 0} \int \frac{d^{d+1}k}{(2\pi)^{d+1}} G_\uparrow(k) G_\uparrow(q+k) - G_\downarrow(k) G_\downarrow(q+k). \quad (9)$$

Hence

$$\Pi_{\text{mix}}^{00} = g_\uparrow(\epsilon_F) - g_\downarrow(\epsilon_F). \quad (10)$$

Note that Π is defined with a negative sign, that is $\Pi = -\mathcal{A}$, where \mathcal{A} is the two-point amplitude. G are the electron Green's functions. $g(\epsilon_F)$ are the densities of states at Fermi energy.

As is well known, the Dyson-Schwinger all-order corrections to a fish diagram such as that indicated in eqn. (6) is incorporated by replacing the Green's functions by their

all-order counterparts and one or the other of the vertices (and not both) by their all-order counterpart. Equation (10) is an all-order expression in the sense that the Green's functions are arbitrary. However, the vertex correction needs care. Let us consider the all-order correction to the photon vertex. At zero external energy and momenta, the time component of the all-order vertex is given by the energy derivative of G^{-1} , by virtue of the Ward–Takahashi identity. It follows that, if the all-order Green's function is given by

$$G(E, \mathbf{k}) = \frac{Z}{E - \epsilon(\mathbf{k}) + i0\text{sgn}(\epsilon(\mathbf{k}) - \mu)}, \quad (11)$$

as is the case for the Fermi liquid, then the vertex is corrected by Z^{-1} . On the other hand, there is Z^2 coming from G^2 , and so the net result is proportional to Z . Z being the correct renormalizing factor for the density of states, eqn. (10) is exact. It is not difficult to see that a more general form of G also admits this property:

$$G(E, \mathbf{k}) = \frac{Z(\mathbf{k})}{f(E - \epsilon(\mathbf{k}) + i0\text{sgn}(\epsilon(\mathbf{k}) - \mu))}, \quad (12)$$

where f is any function, so long as the density of states is definable as the integral of G . Thus it is not a necessary condition that the system is a Fermi liquid.

Returning to eqn. (10), in general, g_\uparrow and g_\downarrow are not equal at the Fermi surface, and therefore the currents mix.

It is worth noting here that the current mixing is zero in the case of anti-ferromagnetism, because the two sublattice contributions are equal and opposite.

Before proceeding, let us calculate the other fish diagrams. Both for the EM current and for the spin $U(1)_z$ current, we obtain:

$$\Pi_{\text{EM}}^{00} = \Pi_z^{00} = g_\uparrow(\epsilon_F) + g_\downarrow(\epsilon_F). \quad (13)$$

Again, this is an exact result provided that the Green's functions are of the form eqn. (12) and the densities of states can be defined as their integrals. Note that although we have retained the subscript 'EM' to refer to electromagnetism, in reality, we are analyzing electrostatics.

2.3 Derivation of the ratio rule

Let us now consider the stability of the ferromagnetic ground state. To do so, a primary condition is the vanishing of the tadpole:



$$\sigma^3 \quad (14)$$

as is required by the condition that there are no terms that are linear in the Higgs field in the effective Lagrangian. In other words, the first derivative of free energy as a function of the magnetic order parameter must vanish when the ground state is stable. We will also need to check that the second derivative is positive. This means the term which is


bilinear in the Higgs field, or the self-energy of the Higgs boson, is positive. The Higgs self-energy is the same as Π_z^{00} calculated earlier on, up to the square of a coupling constant. This is necessarily positive.

Equation (14) is calculated easily, and we obtain

$$\mathcal{A}_z^{\text{tadpole}} = \int \frac{d^{d+1}k}{(2\pi)^{d+1}i} G_\uparrow(k) - G_\downarrow(k) = \rho_\uparrow - \rho_\downarrow. \quad (15)$$

ρ refers to the total density of states of electrons. This is an exact expression since higher-order corrections to the tadpole are taken into account by making G all-order and vertex to be bare. This is always negative if \downarrow is the preferred orientation of spin.

It follows that eqn. (14) by itself is non-zero. However, the currents mix, and we must incorporate the contribution of the photon tadpole, multiplied by the Higgs–photon two-point function which has the same form as Π_{mixing}^{00} calculated in eqn. (10):



$$\quad (16)$$

Now, to make this equation all-order, we must include the screening effect in the photon propagator, and this has the same form as Π_{EM}^{00} calculated in eqn. (13). Altogether, we obtain

$$\mathcal{A}_{\text{photon part}}^{\text{tadpole}} = (\rho_\uparrow + \rho_\downarrow)e \times \frac{(g_\uparrow(\epsilon_F) - g_\downarrow(\epsilon_F))e}{-(g_\uparrow(\epsilon_F) + g_\downarrow(\epsilon_F))e^2}. \quad (17)$$

The two contributions must vanish when added together. Although the charge e appears here, whether one takes the charge carriers to be electrons or holes is a matter of choice, so e can be taken as constant. Hence,

$$\frac{g_\downarrow(\epsilon_F) - g_\uparrow(\epsilon_F)}{g_\downarrow(\epsilon_F) + g_\uparrow(\epsilon_F)} = \frac{\rho_\downarrow - \rho_\uparrow}{\rho_\downarrow + \rho_\uparrow} \quad (18)$$

or,

$$\frac{g_\uparrow(\epsilon_F)}{g_\downarrow(\epsilon_F)} = \frac{\rho_\uparrow}{\rho_\downarrow}. \quad (19)$$

This is our ferromagnetic ratio rule.

In eqn. (18), the left-hand side is often called the spin polarization P , for example in the context of tunnel magnetoresistance. The right-hand side is the magnetic moment $n_B = m/\mu_B$ divided by the number of carriers n , i.e.,

$$P = \frac{n_B}{n}. \quad (20)$$

Note that the definition of n is ambiguous. However, it is a measure of the number of electrons or holes that are actively involved in the formation of ferromagnetic order. As such, one would expect that its order is estimated by the number of carriers in the conduction band. If so, we obtain a simple rule of the thumb:

$$\begin{cases} g_\downarrow > g_\uparrow \text{ (electrons),} \\ g_\downarrow < g_\uparrow \text{ (holes).} \end{cases} \quad (21)$$

element	$g_{\downarrow}/g_{\uparrow}$	$\rho_{\downarrow}/\rho_{\uparrow}$	P	$n = n_B/P$
Fe	2.1 ± 0.2	$2 \sim 2.5$	0.35 ± 0.04	6.3 ± 0.7
Co	7.0 ± 1.5	> 1	0.75 ± 0.04	2.3 ± 0.1
Ni	10 ± 1.5	> 1	0.82 ± 0.03	0.74 ± 0.03

Table 2. Theoretical numbers for $g_{\downarrow}/g_{\uparrow}$ and $\rho_{\downarrow}/\rho_{\uparrow}$. The numbers for g were measured using a ruler applied to the density-of-state plots of ref. [11]. The numbers for ρ were estimated by the eye and a ruler. The Fermi level is at the tail of the density of states for the case of Co and Ni, and rendering the definition of ρ difficult or arbitrary. We also show the values of P corresponding to these values of $g_{\downarrow}/g_{\uparrow}$, and an estimate of n based on the actual values of n_B which are shown in tab. 1.

We also show the values of P calculated from $g_{\downarrow}/g_{\uparrow}$. These are quite different from the experimental numbers introduced earlier. As a result, the numbers for n differ from before, if we use the same values of n_B .

To summarize, it is difficult to check the ratio rules quantitatively, at the present level of accuracy.

2.6 Physical interpretation

Let us discuss tadpole cancellation in a more intuitive fashion.

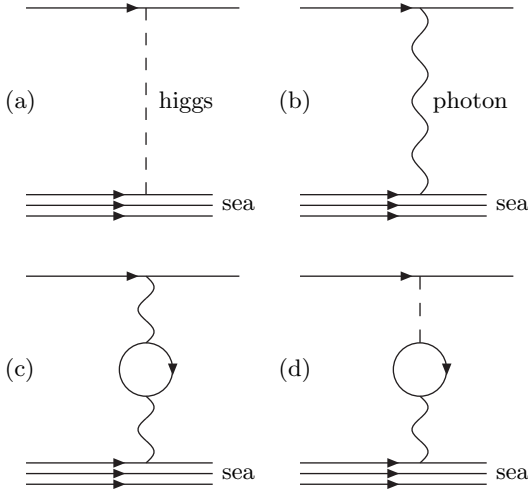


Fig. 1. The interaction of a conduction electron with the Fermi sea of electrons.

Figure 1 represents the interaction experienced by a conduction electron or holes due to the surrounding Fermi sea of (conduction) electrons or holes. Let us say that the charge carriers are electrons. Note that fig. 1a corresponds to eqn. (14), and fig. 1d corresponds to eqn. (16).

The interaction shown in Fig. 1a involves the exchange of the density fluctuation of spin, i.e., the Higgs boson. This boson being a scalar, its exchange is always repulsive between like particles, i.e., between the same spin. Since, by definition, there are more majority-spin electrons than

minority spin electrons, this interaction makes majority-spin electrons more energetically unfavourable. That is, Fig. 1a, or the density fluctuation of spin, tends to suppress magnetic order.

The exchange of the Higgs boson is not the only interaction between the conduction electrons and the sea, and in Fig. 1b, we show the Coulomb exchange. This is always repulsive, and is of the same magnitude for both type of electrons, and so this diagram does not contribute to the formation or suppression of magnetic order.

Figure 1b by itself is infinite since the photon propagator diverges at zero momentum transfer. This is, as usual, remedied by the screening effect which is shown in fig. 1c.

The screening effect, such as that shown in fig. 1c, usually suppresses the charge. This is because a negative charge attracts positive charge, and this positive charge tends to cancel the negative charge.

However, the contribution of fig. 1d requires more thought.

The sea electrons, which have negative charge, attracts positive charge. When this positive charge has the same spin as the conduction electron, i.e., when the positive charge suppresses the electronic spin which is aligned with the spin of the conduction electron, the positive charge attracts this conduction electron. On the other hand, when the positive charge has opposite spin to that of the conduction electron, then the conduction electron is repelled.

Whether the interaction of fig. 1d tends to create magnetic order or suppress it depends on which type of spin is more likely to be excited, i.e., on the density of states at the Fermi surface. This is the meaning of the tadpole cancellation. In other words, the ferromagnetic ground state is stable when the interaction due to the fluctuation of spin density, which is mediated by the Higgs boson and which always suppresses the polarization of spin, is equal and opposite to the contribution due to the electrostatic polarization of fig. 1d which, depending on circumstances, can counteract it.

2.7 Comparison with the Hubbard model

When the Coulomb interaction is screened, the interaction becomes point-like in the limit of large screening, i.e.,

$$\frac{1}{g_{\downarrow}(\epsilon_F) + g_{\uparrow}(\epsilon_F)} \rightarrow \hat{U}, \quad (27)$$

where \hat{U} is a constant which can be interpreted as the on-site Coulomb repulsion U up to a normalization. Let us now see what would happen if we were to start from a theory which treats the on-site Coulomb repulsion U as the starting point, such as the Hubbard model.

In this case, eqn. (14) is unchanged, but eqn. (16) is modified to take the following form:

$$\sigma_{ab}^3 \begin{array}{c} \curvearrowright \\ \curvearrowleft \end{array} \hat{U} \quad (28)$$

Here, as is usual in the Hubbard model, the spin going into the fish part must be opposite to the spin going into

the tadpole. That is,

$$\mathcal{A}_{\text{Hubbard}}^{\text{tadpole}} = \hat{U} [g_{\uparrow}(\epsilon_F)\rho_{\downarrow} - g_{\downarrow}(\epsilon_F)\rho_{\uparrow}], \quad (29)$$

in the place of eqn. (17). This would lead to different consequences.

The origin of this discrepancy is clear. Expressed in terms of the screened Coulomb propagator, there are two contributions that go into eqn. (28). One is the genuine tadpole-like contribution of the form eqn. (16). The contribution of this term is given by

$$\hat{U} [g_{\uparrow}(\epsilon_F) - g_{\downarrow}(\epsilon_F)] (\rho_{\downarrow} + \rho_{\uparrow}), \quad (30)$$

so that this term has the same form as in eqn. (28). On the other hand, there is a second contribution, which is the self-energy correction:



$$\sigma_{ab}^3 \quad (31)$$

The contribution due to this term is given by

$$\hat{U} [g_{\downarrow}(\epsilon_F)\rho_{\downarrow} - g_{\uparrow}(\epsilon_F)\rho_{\uparrow}]. \quad (32)$$

Adding together these two contributions yields eqn. (29).

The discrepancy comes because in our approach, the self-energy correction is absorbed in the all-order Green's function, whereas in the Hubbard-model approach, this is not possible. In the Hubbard model, either both contributions are treated as a tadpole, or both contributions are treated as a self-energy correction. If the latter, one will have the condition that the simple tadpole, with the self-energy corrections, by itself vanishes. This condition requires $\rho_{\uparrow} = \rho_{\downarrow}$, and therefore we will never have a stable ferromagnetic solution out of the Hubbard model.

This, in our opinion, is a limitation of the Hubbard model. The limitation is due to the inability to treat current-current mixing, which is the basis of our discussion in this section.

One may still argue that on-site Coulomb repulsion is present, physically. In other words, the effective screened Coulomb propagator, which ordinarily gives a divergent contribution at the origin up to a UV cut-off, is not really divergent but only large and finite at the origin.

If so, this may be thought of as a variant of the UV cut-off of the Coulomb propagator D_{photon} , which may be parametrized, for example, as

$$D_{\text{photon}}(\mathbf{k}) = \frac{1}{-\mathbf{k}^2 - a\mathbf{k}^4}, \quad (33)$$

where a is a parameter (positive or negative). Even if this is not permissible as a field theory, it is permissible as an UV (Pauli–Villars) regularization procedure. It will be seen that such a cut-off does not affect our argument at all, since our discussion involves zero momentum photons. The electron self-energy will be affected by the UV cut-off, but this does not affect our results explicitly.

3 Analysis of spin current conservation

Let us now move on to the formalism, which is required if we are to go beyond the tadpole-level analysis of the preceding section. We adapt Gribov's analysis of axial current conservation [2,3] to the context of spin current conservation in systems with partial magnetic order.

To sum up in one phrase, our goal is to start from the Coulombic system, which is defined by eqn. (2), and solve it as exactly as possible using the Dyson–Schwinger equations, under a number of assumptions.

The major assumption is that of spontaneous symmetry breaking. If the spin symmetry is broken spontaneously, then the Goldstone theorem guarantees the presence of Goldstone and Higgs modes. These modes are, in terms of the initial Lagrangian, electronic excitations. However, in terms of the effective theory that appears at the end, they are elementary, and participate in the conservation of the spin current. This is the main property that allows us to solve the Dyson–Schwinger equations. The other assumptions, such as the linear or quadratic form of the magnon dispersion relation and the constancy of exchange energy which are sometimes required, are approximations, which we believe are viable, that can be lifted if one has the computational resources.

The resulting effective Lagrangian is found to have the following interaction term:

$$\mathcal{L}_{\text{eff}}^{\text{I}} \propto \psi^{\dagger} \Phi \cdot \sigma \psi. \quad (34)$$

Here Φ^i is essentially the order-parameter field, but with a certain formal difference which we shall discuss. We would like to emphasize at this point that this equation is not our starting point. It is rather the end product of solving the Coulombic system by means of the Dyson–Schwinger equations, with the aid of the Goldstone theorem and the Ward–Takahashi identities.

Let us start by discussing current conservation. As discussed in the previous section, current is absolutely conserved when the spin symmetry is conserved.

$$\frac{\partial}{\partial x^{\mu}} J_{\text{spin}}^{\mu,i} = 0. \quad (35)$$

Current conservation is reflected in the following Ward–Takahashi identity:

$$\Gamma^{\mu}(q_1 - q_2)_{\mu} = G_{\lambda_1}^{-1}(q_1) - G_{\lambda_2}^{-1}(q_2). \quad (36)$$

Γ^{μ} is the vertex in the momentum space. $\lambda_{1,2}$ refer to the spin states, but these are dummy indices here in the sense that $G_{\lambda}^{-1}(q)$ is independent of λ . Thus eqn. (36) holds for any combination of spin, and therefore current is conserved. q are $d+1$ -vectors with components (q_0, \mathbf{q}) . q_0 is the energy and \mathbf{q} is the spatial momentum, with $\hbar = 1$.

The Ward–Takahashi identity is violated in the symmetry-broken phase, since there is now an energy difference ΔE , which is the exchange energy, between the different spin states:

$$\Delta E = G_{\downarrow}^{-1}(q) - G_{\uparrow}^{-1}(q). \quad (37)$$

For example, for the configuration of fig. 2a, eqn. (39) yields the following Ward–Takahashi identity:

$$q^\mu \Gamma_\mu + i^2 (-f D_\phi^{-1}(q)) D_\phi(q) (f^{-1} \Delta E) = G_-^{-1} - G_+^{-1}. \quad (42)$$

Note that the same Feynman rules can be obtained, less rigorously, by considering the rotation associated with the Goldstone bosons, eqn. (40), and considering its coupling with the fermions in eqn. (2).

The vertices that involve the Higgs boson, which are shown in fig. 2c and d, cannot be fixed by this particular type of Ward–Takahashi identity. However, they can be fixed by considering the current insertion in the three-point amplitude, for example, as shown in fig. 3.

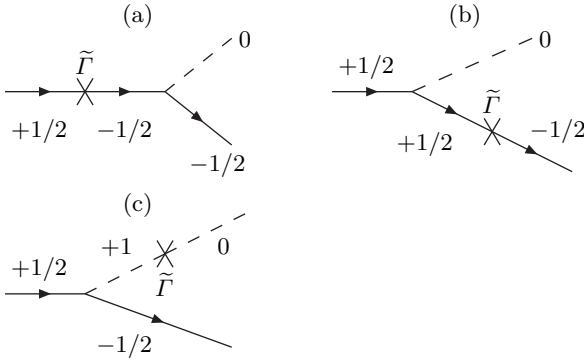


Fig. 3. The three diagrams whose sum must satisfy the Ward–Takahashi identity. The crosses correspond to the modified current vertex defined by eqn. (39).

The Ward–Takahashi identity applied to fig. 3 also allows us to determine the magnon–magnon–Higgs vertex. However, for doing so, we need to know the form of $D_\phi(q)$ and $D_h(q)$. Let us therefore calculate the current–magnon two-point function of eqn. (41).

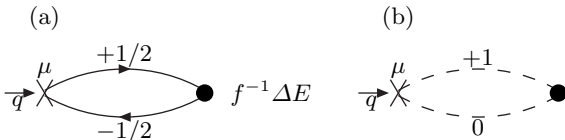


Fig. 4. The fermionic (a) and bosonic (b) contributions to the current–magnon two-point function.

For now, we calculate the fermionic loop, which is shown in fig. 4a. It should be noted that the end result of this calculation is independent of whether we consider ϕ_+ or ϕ_- . Using the Feynman rule of fig. 2a, we obtain

$$i\mathcal{A}_{\text{two-point}}^\mu(q) = i^4 (-1) \int \frac{d^{d+1}k}{(2\pi)^{d+1}} \Gamma^\mu G_+(k) G_-(k-q) (f^{-1} \Delta E). \quad (43)$$

In particular, for the case $q \rightarrow 0$, we obtain the exact expression:

$$\mathcal{A}_{\text{two-point}}^\mu(q \rightarrow 0) = \int \frac{d^{d+1}k}{(2\pi)^{d+1}} f^{-1} \Gamma^\mu [G_-(k) - G_+(k)], \quad (44)$$

where we made use of eqn. (37). For Fermi liquids, $\Gamma^0 = 1$ and, by symmetry, the spatial components of this amplitude usually vanishes at $q = 0$. We thus obtain

$$\mathcal{A}_{\text{two-point}}^\mu(q \rightarrow 0) = f^{-1} (\rho_- - \rho_+, 0, 0, 0). \quad (45)$$

Note that this vanishes for the case of anti-ferromagnetism where there is no global spin asymmetry.

When we compare eqn. (45) with eqn. (41), we see immediately that

$$f^2 = \rho_- - \rho_+ \quad (\text{ferromagnetism}), \quad (46)$$

and

$$\begin{cases} -D_\phi^{-1}(q) = q_0 - \mathbf{q}^2/2m_\phi & (\text{ferromagnetism}), \\ -D_\phi^{-1}(q) = q_0^2 - u^2 \mathbf{q}^2 & (\text{anti-ferromagnetism}), \end{cases} \quad (47)$$

for small energy and momenta. The inclusion of the bosonic loop does not alter this conclusion. The unusual negative sign of D reflects the fact that the magnons are pseudoscalar. That is, the fields are $i\phi$ rather than ϕ in our convention.

We need to calculate f^2 by other means, such as calculating the two-point amplitude for finite q , for anti-ferromagnetism. u and m_ϕ are parameters which are in principle calculable by, for example, evaluating the finite q case. However, the form of eqn. (43) implies $m_\phi \sim m_e$ and $u \sim v_F$.

There is actually a smarter method than to calculate the finite- q case (which is cumbersome), but the full calculation, in the case of anti-ferromagnetism, requires our knowledge of the bosonic three-point functions. Let us therefore postpone the calculation of anti-ferromagnetic f^2 and other parameters for now.

Let us summarize the results of this section up to here.

Firstly, we summarize the propagators and the two-point functions in fig. 5. The Higgs-boson Green's functions are given in fig. 5b, with a constant energy gap Δ_h . Δ_h is defined as the energy gap for ferromagnetism and the energy gap squared for anti-ferromagnetism. This definition is convenient when we discuss the bosonic three-point functions. Note that it is an approximation to say that Δ_h is independent of momenta and energy. However, it becomes easier to implement current conservation in this manner. For completeness's sake, we also list the screened photon Green's function (with the approximation that the screening, Π_{EM} , is constant) and the Higgs–photon mixing. These are as given in the previous section.

Secondly, the fermionic vertices are as given before in fig. 2. We did not list the photonic vertex, but this is given by e . Note that the couplings given in fig. 2 can be summarized in the following compact form (c.f. eqn. (34)):

$$\mathcal{L}_{\text{eff}}^{\text{I}} = (f^{-1} \Delta E) \psi^\dagger \Phi \cdot \sigma \psi, \quad (48)$$

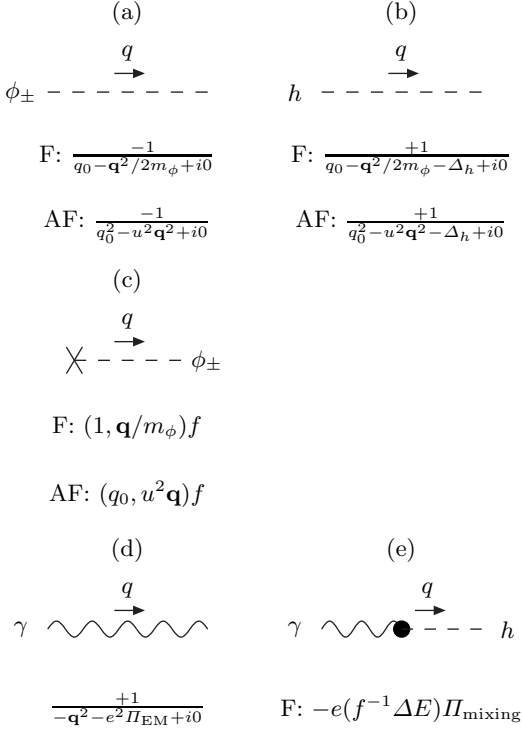


Fig. 5. The propagators and the two-point functions. Π_{EM} is given by the $0-0$ component of eqn. (13), and Π_{mixing} is given by the $0-0$ component of eqn. (10).

where Φ is defined by

$$\Phi = (\phi_1, \phi_2, -v + h). \quad (49)$$

ϕ_1 and ϕ_2 are as shown in tab. 3, and are given by

$$\phi_1 = \frac{1}{2}(-\phi_+ + \phi_-), \quad \phi_2 = \frac{i}{2}(\phi_+ + \phi_-). \quad (50)$$

v is a parameter, which has the interpretation as the vacuum expectation value of the Φ field. In order that the energy difference between the two states that is given by eqn. (48) should agree with the actual energy difference ΔE , v needs to satisfy

$$v = f/2. \quad (51)$$

Φ is essentially a magnetic order-parameter field. This differs from the more conventional form such as

$$\mathcal{U}(\phi_1, \phi_2)(0, 0, v + h)^T, \quad (52)$$

but they match in the limit of small fields, up to some differences in convention.

3.2 Bosonic vertices

Let us consider the Ward–Takahashi identity corresponding to the amplitude described by fig. 3.

We denote the initial state momentum to be q_1 and the final state momenta to be q_2 and q_3 . q_2 is for the h_0 boson

and q_3 is for the $-1/2$ fermion. We denote the momentum which goes into the vertex by q , so that $q + q_1 = q_2 + q_3$. It is not necessary that the fermions and the bosons are on shell, i.e., $G_+^{-1}(q_1)$ etc. need not be zero.

Upon contraction with q , the first two diagrams yield

$$q_\mu \mathcal{A}_a^\mu = -i^2 f^{-1} \Delta E (1 - G_+^{-1}(q_1) G_-(q + q_1)) \quad (53)$$

and

$$q_\mu \mathcal{A}_b^\mu = i^2 f^{-1} \Delta E (G_-^{-1}(q_3) G_+(q_3 - q) - 1). \quad (54)$$

The amplitude as a whole satisfies the Ward identity if the third amplitude satisfies

$$q_\mu \mathcal{A}_c^\mu = 2i^2 f^{-1} \Delta E (1 + D_h^{-1}(q_2) D_\phi(q_2 - q)). \quad (55)$$

This requires vertices of the form shown in fig. 6.

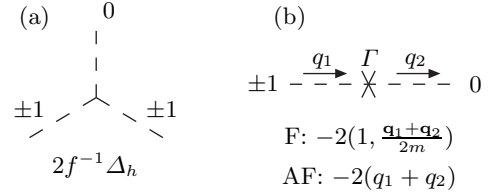


Fig. 6. The bosonic three-point functions. In (b), $q_1 + q_2$ is a short-hand notation for $((q_1 + q_2)_0, u^2(\mathbf{q}_1 + \mathbf{q}_2))$.

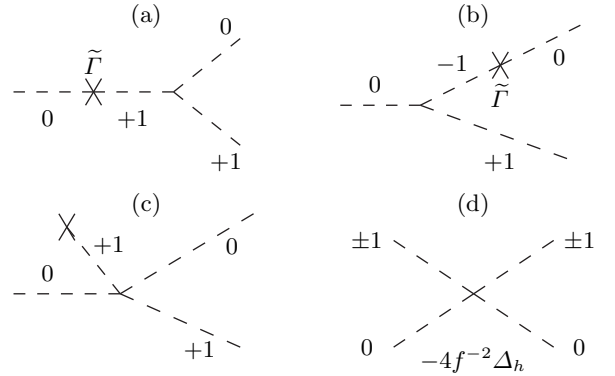


Fig. 7. The three diagrams (a–c) whose sum must satisfy the Ward–Takahashi identity. The bosonic four-point function (d) is fixed as a result.

Finally, we require the Ward–Takahashi identity for the sum of the three diagrams which are shown in fig. 7a–c. We choose the momenta to be $h(q_1) \rightarrow h(q_2) + \phi_+(q_3)$, with $q = q_2 + q_3 - q_1$ being the four-momentum flowing into the current. We obtain

$$q_\mu \mathcal{A}_a^\mu = -4i^2 f^{-1} \Delta_h (D_h^{-1}(q_1) D_\phi(q_1 + q) + 1), \quad (56)$$

and

$$q_\mu \mathcal{A}_b^\mu = -4i^2 f^{-1} \Delta_h (D_h^{-1}(q_2) D_\phi(q_2 - q) + 1). \quad (57)$$

Thus we require

$$q_\mu \mathcal{A}_c^\mu = 8i^2 f^{-1} \Delta_h \quad (58)$$

in order that the Ward–Takahashi identity is satisfied. Hence we obtain the Feynman rule shown in fig. 7d.

4 Calculation of the parameters

In the preceding section, we worked out the form of the theory. Let us now work out the parameters.

In sec. 2, we used the condition of tadpole cancellation to work out a certain rule involving the ratios of density of states, that need to be satisfied in ferromagnetism.

In sec. 3, we presented the Feynman rules and were able to relate the current–magnon two-point function to the form of f^2 and the bosonic propagators.

We now generalize these results, and work out the four parameters, which are (1) f^2 , (2) ΔE , (3) Δ_h and (4) u or m_ϕ .

Corresponding to these four unknowns, we have four equations, which involve: (1) tadpole cancellation, (2) the time component of the current–boson two-point function, (3) the space component of the same two-point function and (4) the Higgs-boson self-energy.

4.1 Tadpole cancellation

Let us start with the condition of tadpole cancellation.

We treated the ferromagnetic case in sec. 2. The anti-ferromagnetic case is calculated analogously, but the mechanism of cancellation is different. This time, we have the contribution of the magnon loop:

$$i\mathcal{A}_{\text{magnon}}^{\text{tadpole}} = i^2(2f^{-1}\Delta_h) \int \frac{d^{d+1}k}{(2\pi)^{d+1}} D_\phi(k), \quad (59)$$

which must be equal and opposite to the fermionic loop:

$$i\mathcal{A}_{\text{fermion}}^{\text{tadpole}} = (-1)i^2(f^{-1}\Delta E) \int \frac{d^{d+1}k}{(2\pi)^{d+1}} (G_+(k) - G_-(k)). \quad (60)$$

Note that the sum over positive and negative ΔE is implicit.

This gives us the following condition:

$$-2\Delta_h \int \frac{d^{d+1}k}{(2\pi)^{d+1}} D_\phi(k) = \sum_{\text{sublattices}} [(\rho_+ - \rho_-)\Delta E]. \quad (61)$$

Note that ΔE is positive when $\rho_- > \rho_+$. That is, the right-hand side is negative. Let us introduce a more compact notation:

$$2\Delta_h \int D_\phi = \rho_M |\Delta E|. \quad (62)$$

The convention is that $\rho_M = \sum |\rho_- + \rho_+|$ is positive. The integral of D_ϕ is evaluated easily:

$$\int D_\phi = \int \frac{d^{d+1}k}{(2\pi)^{d+1}} \frac{-1}{k_0^2 - u^2 \mathbf{k}^2 + i0} = \int \frac{d^d \mathbf{k}}{2u(2\pi)^d |\mathbf{k}|}. \quad (63)$$

This is divergent at large momenta, and needs to be cut-off at $|\mathbf{k}| = K$, where $K \sim \pi/a$. We then obtain

$$\frac{\rho_M |\Delta E|}{2\Delta_h} = \begin{cases} K/4\pi u & (d=2), \\ K^2/8\pi^2 u & (d=3). \end{cases} \quad (64)$$

Note that the propagators are all-order, and this requires that ΔE is bare, and that the vertex corrections are not included in eqn. (59). Whether ΔE is stable against higher-order corrections depends on the size of the coupling $f^{-1}\Delta E$ and the relative size of u compared with the electron velocity $v \approx v_F$. The form of eqn. (59) corresponds to the all-order vertex, and therefore this equation, and eqn. (64) which follows from it, suffer from double counting. However, this ambiguity, that is due to double counting, cancels when we discuss the Higgs-boson self-energy later on.

4.2 Current–magnon two-point function

In sec. 3, we calculated the fermionic contribution to the current–magnon two-point function, which is shown in fig. 4a. We obtained

$$\mathcal{A}_{\text{fermionic}}^\mu = - \int \frac{d^{d+1}k}{(2\pi)^{d+1}} (f^{-1}\Delta E) \Gamma^\mu G_+(k) G_-(k-q). \quad (65)$$

For the simple case of $\epsilon(\mathbf{k}) = (\hbar\mathbf{k})^2/2m_e$, the vertex is given by $\Gamma^\mu = (1, (\mathbf{k} - \mathbf{q}/2)/m_e)$. The bosonic loop, which corresponds to fig. 4b, is written as

$$\mathcal{A}_{\text{bosonic}}^\mu = \int \frac{d^{d+1}k}{(2\pi)^{d+1}} (2f^{-1}\Delta_h) (-2(2k-q)) D_h(k) D_\phi(k-q) \quad (66)$$

This is for the anti-ferromagnetic case. Note that the case of ferromagnetism requires a further twist, as we have not yet included the higgs–screened-photon mixing.

Let us consider the limit of small external momentum, $q \rightarrow 0$. It is easy to see that the fermionic amplitude vanishes for anti-ferromagnetism. As for the bosonic amplitude, this vanishes for ferromagnetism because of the absence of negative energy states. The amplitude vanishes for anti-ferromagnetism also, but for a different reason, namely symmetry.

Let us, instead of trying to evaluate these integrals for arbitrary values of q , make use of the Ward–Takahashi identities to replace the current–magnon two-point functions with the corresponding current–current two-point functions (c.f., ref. [2]).

To do so, we first write down the current–current two-point functions as

$$\Pi_{\text{fermionic}}^{\mu\nu} = - \int \frac{d^{d+1}k}{(2\pi)^{d+1}} \Gamma^\mu \Gamma^\nu G_+(k) G_-(k-q), \quad (67)$$

and

$$\Pi_{\text{bosonic}}^{\mu\nu} = \int \frac{d^{d+1}k}{(2\pi)^{d+1}} (-2(2k-q)^\mu) (-2(q-2k)^\nu) D_h(k) D_\phi(k-q). \quad (68)$$

By virtue of the Ward–Takahashi identities, we obtain

$$q_\nu \Pi^{\mu\nu} - f \mathcal{A}^\mu = C_{\text{fermionic}}^\mu + C_{\text{bosonic}}^\mu, \quad (69)$$

where C^μ are given by

$$C_{\text{fermionic}}^\mu = \int \frac{d^{d+1}k}{(2\pi)^{d+1}i} \Gamma^\mu(k, q-k) (G_+(k) - G_-(k-q)) \quad (70)$$

and

$$C_{\text{bosonic}}^\mu = \int \frac{d^{d+1}k}{(2\pi)^{d+1}i} (-2(2k-q)^\mu) (D_h(k) + D_\phi(k-q)). \quad (71)$$

We now equate \mathcal{A} with the Feynman rules of fig. 5c, and take the derivative with respect to q_λ in the limit of small q . For the ferromagnetic case, we obtain

$$\Pi_{\text{fermionic}}^{\mu\lambda} \Big|_{q \rightarrow 0} + f^2 m_\phi^{-1} \text{diag}(0, -I) = \frac{\partial}{\partial q_\lambda} C_{\text{fermionic}}^\mu \Big|_{q \rightarrow 0}. \quad (72)$$

I stands for the spatial identity matrix. The $0-0$ component of this equation is zero on the right-hand side and in the second term of the left-hand side, whereas the first term on the left-hand side is non-zero:

$$\Pi_{\text{fermionic}}^{00} \Big|_{q \rightarrow 0} = - \int G_+ G_- = \frac{\rho_- - \rho_+}{\Delta E}. \quad (73)$$

This happens because of the approximation $D_\phi^{-1}(q) = q_0 - \mathbf{q}^2/2m_\phi$. There is, in principle, a q_0^2 term as well, the omission of which is inconsistent with the $0-0$ component of this equation. As for the spatial components, we obtain

$$f^2 m_\phi^{-1} d = \int \frac{d^{d+1}k}{(2\pi)^{d+1}i} \left[(G_+(k) + G_-(k)) \frac{d}{2m_e} + G_+(k) G_-(k) v_e^2 \right]. \quad (74)$$

Here, d/m_e refers to the second derivative of $\epsilon(k)$, whereas v_e refers to the first derivative.

Let us introduce the following shorthand notation:

$$f^2 m_\phi^{-1} = \left\langle \frac{\rho_- + \rho_+}{2m_e} - \frac{(\rho_- - \rho_+) v_e^2}{\Delta E d} \right\rangle. \quad (75)$$

There is an obvious generalization to the case of spatial asymmetry. We expect this final result to be stable against higher-order corrections, because the renormalization factors due to the vertex correction and the Green's functions cancel.

As discussed in sec. 2, $(\rho_- + \rho_+)$ is not well-defined. However, the ratio of $(\rho_- + \rho_+)$ against $(\rho_- - \rho_+)$ is well defined because of eqn. (18). Furthermore, f^2 is given by $\rho_- - \rho_+$.

As an order estimation, we can say that v_e can be taken to be almost constant near the Fermi surfaces. It would be a bad approximation to say that m_e is also constant,

but we can introduce a quantity $\overline{m_e}$ to be the inverse of the average inverse fermion mass. We then obtain

$$\frac{2\overline{m_e}}{m_\phi} \approx \frac{1}{P} - \frac{2\overline{m_e} v_F^2}{\Delta E d}. \quad (76)$$

P is the spin asymmetry. m_ϕ is necessarily positive, but $\overline{m_e}$ needs not be positive although we generally expect it to be. If $\overline{m_e}$ is positive, then the inequality reads

$$P \lesssim \frac{\Delta E d}{2\overline{m_e} v_F^2}. \quad (77)$$

Let us now turn to the anti-ferromagnetic case. Here we need both the fermionic and the bosonic loops. Corresponding to eqn. (72), we now have

$$\Pi^{\mu\lambda} \Big|_{q \rightarrow 0} + f^2 \text{diag}(1, -u^2 I) = \frac{\partial}{\partial q_\lambda} C^\mu \Big|_{q \rightarrow 0}. \quad (78)$$

The fermionic contributions are as given above. The bosonic contributions are given by

$$\Pi_{\text{bosonic}}^{\mu\lambda} \Big|_{q \rightarrow 0} = -16 \int k^\mu k^\lambda D_h D_\phi, \quad (79)$$

and

$$\frac{\partial}{\partial q_\lambda} C_{\text{bosonic}}^\mu = 2 \text{diag}(1, -u^2 I) \int D_h - D_\phi, \quad (80)$$

using the same notation as in eqn. (62). The integral over D_ϕ is given by eqn. (63), and is a positive quantity. The integral over D_h is given by

$$\int D_h = - \int \frac{d^d \mathbf{k}}{2(2\pi)^d \sqrt{u^2 \mathbf{k}^2 + \Delta_h}}, \quad (81)$$

and this is a negative quantity.

Altogether, we obtain

$$f^2 + 2 \int (D_h - D_\phi) - 16 \int k_0^2 D_h D_\phi = - \frac{\rho_M}{|\Delta E|}, \quad (82)$$

and

$$\begin{aligned} f^2 + 2 \int (D_h - D_\phi) - \frac{16}{d} \int \mathbf{k}^2 D_h D_\phi \\ = \frac{1}{u^2} \left\langle \frac{\rho_- + \rho_+}{2m_e} - \frac{\rho_M v_e^2}{|\Delta E| d} \right\rangle. \end{aligned} \quad (83)$$

4.3 The Higgs-boson self-energy

We now come to the final condition, namely that the Higgs-boson excitation energy Δ_h is given by the self-energy diagrams which are shown in fig. 8.

The fermionic contribution is similar to Π_z^{00} which was calculated in sec. 2, and is given by

$$\begin{aligned} -i\Pi_a^h = -i^4 \int \frac{d^{d+1}k}{(2\pi)^{d+1}} (f^{-1} \Delta E)^2 \\ (G_+(k) G_+(k-q) + G_-(k) G_-(k-q)). \end{aligned} \quad (84)$$

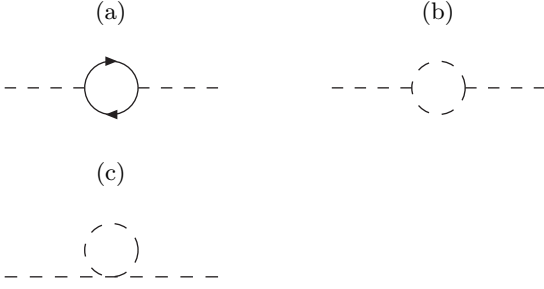


Fig. 8. The diagrams for the self-energy of the Higgs boson.

Hence

$$\Pi_a^h = (f^{-1}\Delta E)^2 (g_-(\epsilon_F) + g_+(\epsilon_F)). \quad (85)$$

Note that ΔE refers to the bare quantity. This is because, firstly, $(\Delta E)^2$ in eqn. (84) needs to be the product of the bare ΔE and the renormalized ΔE . However, the renormalization of ΔE gives rise to the renormalization factor Z^{-1} which is opposite to the renormalization factor Z for each propagator. It follows, therefore, that ΔE in eqn. (85) actually refers to the bare quantity.

At $q = 0$ (and at zero temperature), the contributions of fig. 8b and c are zero for ferromagnetism. Hence, for the case of ferromagnetism, we obtain

$$\Delta_h = \frac{g_-(\epsilon_F) + g_+(\epsilon_F)}{\rho_- - \rho_+} (\Delta E)^2. \quad (86)$$

If the density of states g is a linear function, then $\Delta_h = 2\Delta E$ since $(\rho_- - \rho_+)$ is given by the area of a trapezium whose two parallel sides are g_- and g_+ , and whose height is ΔE . If not, and g is a convex function in between g_- and g_+ as is the case for iron [11], Δ_h will be less than $2\Delta E$. This gives a useful estimate of the Higgs-boson excitation energy, which can be tested experimentally.

We should remember that the Higgs-screened-photon mixing cannot be neglected when the spin asymmetry P is large. The actual value of Δ_h where the resonance occurs will be sensitive to the behaviour of the photonic modes (screened photon and plasmon).

Let us now turn to anti-ferromagnetism. The contribution of fig. 8b is given by

$$-i\Pi_b^h = i^4 \int \frac{d^{d+1}k}{(2\pi)^{d+1}} (2f^{-1}\Delta_h)^2 D_\phi(k) D_\phi(k-q). \quad (87)$$

This is divergent, but is imaginary at zero temperature for $q_0^2 - u^2 \mathbf{q}^2 > 0$ (which is where the Higgs mode needs to exist). We therefore omit this contribution for now. The contribution of fig. 8c is given by

$$-i\Pi_c^h = i^2 \int \frac{d^{d+1}k}{(2\pi)^{d+1}} (-4f^{-2}\Delta_h) D_\phi(k). \quad (88)$$

Now using eqn. (62), this reduces to

$$\Pi_c^h = -4f^{-2}\Delta_h \int D_\phi(k) = -2f^{-2}\rho_m |\Delta E|. \quad (89)$$

Hence,

$$\begin{aligned} \Delta_h &= \Pi_a^h + \Pi_c^h \\ &= 2f^{-2} |\Delta E| \left[\frac{1}{2} (g_-(\epsilon_F) + g_+(\epsilon_F)) |\Delta E| - \rho_m \right]. \end{aligned} \quad (90)$$

We thus obtain the anti-ferromagnetic ratio rule:

$$\frac{g_-(\epsilon_F) + g_+(\epsilon_F)}{2\rho_m / |\Delta E|} > 1. \quad (91)$$

This is satisfied if the density of states is a concave function in between the two Fermi energies.

Let us denote the concavity by δ_c , defined as:

$$\delta_c = \frac{g_-(\epsilon_F) + g_+(\epsilon_F)}{2\rho_m / |\Delta E|} - 1. \quad (92)$$

This then leads to

$$\frac{2\rho_m |\Delta E|}{\Delta_h} = \delta_c^{-1} f^2. \quad (93)$$

By eqn. (64), we then obtain

$$f^2 = \begin{cases} \delta_c K / \pi u & (d=2), \\ \delta_c K^2 / 2\pi^2 u & (d=3). \end{cases} \quad (94)$$

Small δ_c therefore leads to strong coupling $f^{-1}\Delta E$. We expect physically that strong coupling tends to suppress magnetism, because the oscillations between the two spin states will become more frequent. Our results are not affected so long as the densities of states can be defined. However, ΔE will receive a large correction through the electron self-energy.

4.4 Summary of results at zero temperature

Let us summarize our results.

For the case of ferromagnetism, the parameters ΔE , f^2 , m_ϕ and Δ_h are fixed by the following constraints:

$$\rho_+ / \rho_- = g_+(\epsilon_F) / g_-(\epsilon_F), \quad (95)$$

$$f^2 = \rho_- - \rho_+, \quad (96)$$

$$f^2 m_\phi^{-1} = \left\langle \frac{\rho_- + \rho_+}{2m_e} - \frac{(\rho_- - \rho_+) v_e^2}{\Delta E d} \right\rangle, \quad (97)$$

$$f^2 \Delta_h = (g_-(\epsilon_F) + g_+(\epsilon_F)) (\Delta E)^2. \quad (98)$$

Out of these equations, which are all non-perturbative, the first three are relations that only involve all-order quantities. In the last equation, ΔE refers to the bare quantity. In eqn. (97), ΔE is the all-order quantity, but is assumed to be more or less independent of energy and momenta (though generalization is possible).

For the case of anti-ferromagnetism, $|\Delta E|$, f^2 , u and Δ_h are fixed by eqns. (64), (82), (83) and (93). Equations (64) and (93) involve $|\Delta E|$ as a bare quantity and Δ_h in eqn. (93) is ambiguous. Equations (82) and (83) only involve all-order quantities, but are dependent on the UV cut-off, as is the case in eqn. (64).

We obtained the rule $\delta_c > 0$, where δ_c is a measure of concavity and is defined by eqn. (92).

4.5 Finite temperature analysis

Since our results involve diagrams that are evaluated for $q = 0$, it is, in principle, straightforward to generalize them to finite temperatures. However, the bosonic diagrams, which were zero in the case of ferromagnetism, become non-zero at finite temperatures, and therefore the resulting expressions are messy.

A full calculation is beyond the scope of this present analysis, but let us present two representative results.

First, for the case of anti-ferromagnetism, we have found that the bosonic loop of fig. 8b is real and diverges for finite T :

$$\Pi_b^h(T) = -\frac{(2f^{-1}\Delta_h)^2}{32T^3} \int \frac{d^d\mathbf{k}}{(2\pi)^d} \frac{d}{dx} \left(-\frac{\coth(x)}{x} \right) \Big|_{x=u|\mathbf{k}|/2T} \quad (99)$$

This makes Δ_h negative, and so magnetic order is forbidden. In our opinion, this implies that in anti-ferromagnetic metals, a genuine long-range order is not permitted, at least at finite temperatures.

Second, let us consider how the ratio rule of eqn. (18) is modified at finite temperatures. We now have the bosonic contribution which reads

$$\mathcal{A}_{\text{boson}}^{\text{tadpole}}(T) = -(2f^{-1}\Delta_h) \int \frac{d^d\mathbf{k}}{(2\pi)^d} \frac{1}{\exp((\mathbf{k}^2/2m_\phi)/T) - 1}. \quad (100)$$

This is evaluated easily using standard methods. For the case of three spatial dimensions, we obtain

$$\mathcal{A}_{\text{boson}}^{\text{tadpole}}(T) = -2f^{-1}\Delta_h \zeta(3/2) \left(\frac{m_\phi T}{2\pi} \right)^{3/2}. \quad (101)$$

Here, $\zeta(3/2) = 2.612\dots$. This contribution should be equal and opposite to the fermionic contributions, which are given by

$$\mathcal{A}_{\text{fermion}}^{\text{tadpole}}(T) = (f^{-1}\Delta E) [-(\rho_\downarrow - \rho_\uparrow)_T + (\rho_\downarrow + \rho_\uparrow)_T P(T)]. \quad (102)$$

Here ρ and P correspond to their finite-temperature counterparts:

$$\rho_T = \int f((\epsilon - \mu)/T) g(\epsilon) d\epsilon, \quad (103)$$

$$g_T = - \int f'((\epsilon - \mu)/T) g(\epsilon) d\epsilon, \quad (104)$$

where f is the Fermi distribution function. Hence

$$-(\rho_\downarrow - \rho_\uparrow)_T + (\rho_\downarrow + \rho_\uparrow)_T P(T) = 2\zeta(3/2) \left(\frac{m_\phi T}{2\pi} \right)^{3/2} \frac{\Delta_h}{\Delta E}. \quad (105)$$

Δ_h , m_ϕ and ΔE are also functions of temperature.

For small T , we can assume that only the first term on the left-hand side depends significantly on T , and that the parameters on the right-hand side can be taken as constants. This then implies that the magnetization goes down as $T^{3/2}$, which is a well-known result. All of the parameters on the right-hand side are, in principle, measurable. This can then be tested experimentally.

5 Conclusions and Outlook

We presented a nonperturbative framework for treating magnetic order in metals, caused by a Coulomb interaction (or generalized Coulomb interaction).

We obtained interesting ‘ratio rules’ involving the densities of states for both ferromagnetic and anti-ferromagnetic cases. These involve all-order quantities (with the exception of $|\Delta E|$) and can therefore be compared directly with the experimental numbers, if they become available at greater precision.

We have seen that the shape of the density-of-states curve play an essential role in determining the possibility of magnetic ordering. The density of states must rise with energy, when the charge carriers are electrons, for ferromagnetism.

For anti-ferromagnetism, the density-of-states curve must be concave. However, we have seen that the radiative corrections, due to the magnons, at finite temperatures breaks long-range orders. In our understanding, this means that genuine long-range anti-ferromagnetic order is not possible, at least at finite temperatures. More work is required to elucidate the nature of the ground state.

The case of magnetic insulators is not covered by this work, in which the exchange energy ΔE is considered to be more or less independent of \mathbf{k} .

Two cases require special attention, which we have not been able to discuss in much detail. The first is the case of strong coupling, which occurs when f , or the vacuum-expectation value v of the magnetic order-parameter field, is small. Here, we expect that the radiative corrections suppress the magnetic order and that the system will favour the paramagnetic state. The second is the case of large magnon velocity u , in comparison with the electron velocity v_F , in the case of anti-ferromagnetism. Here, the response of the magnetic background becomes instantaneous towards the movement of the electron. We hope to be able to discuss this case in a separate publication [14]

The results of this work can be used to calculate arbitrary amplitudes, such as scattering amplitudes.

The methods presented in this work, being an adaptation of Gribov’s analysis of axial-current conservation, is of a general nature. However, we are presently unaware of other possible applications of the methods presented herein.

We thank I. Hase, S. Sharma, K. Yamaji and T. Yanagisawa for extensive and informative comments and discussions.

We have been informed by Dr. I. Hase that a phenomenological study of the correlation between densities of states of a material and its magnetic properties has previously been reported. However, we have not been able to locate this study.

References

1. See, for example: H. Neuberger and T. Ziman, Phys. Rev. **B 39** (1989) 2608; H. Leutwyler, Phys. Rev. **D 49** (1994) 3033.

2. V. N. Gribov, Eur. Phys. J. **C 10** (1999) 71 [arXiv:hep-ph/9807224]; *ibid.* **10** (1999) 91 [arXiv:hep-ph/9902279].
3. V. N. Gribov, Phys. Lett. **B 336** (1994) 243 [arXiv:hep-ph/9407269].
4. V.N. Gribov, *Orsay lectures on confinement*, arXiv:hep-ph/9403218, arXiv:hep-ph/9407269, arXiv:hep-ph/9905285.
5. For a review, see: Yu.L. Dokshitzer and D.E. Kharzeev, hep-ph/0404216.
6. Y. Nambu and G. Jona-Lasinio, Phys. Rev. **122** (1961) 345; Phys. Rev. **124** (1961) 246.
7. G. Cvetič, Rev. Mod. Phys. **71** (1999) 513.
8. See, for example: D. P. Young, et al., Nature **397** (1999) 412, and references therein.
9. P. M. Tedrow and R. Meservey, Phys. Rept. **238** (1994) 173.
10. R. J. Soulen Jr., et al., Science **282** (1998) 85.
11. R. Maglic, Phys. Rev. Lett. **31** (1973) 546; K. C. Wong, E. P. Wohlfarth and D. M. Hum, Phys. Lett. **A 29** (1969) 452; J. Callaway and C. S. Wang, Phys. Rev. **B 7** (1973) 1096.
12. C. Kittel, *Introduction to solid state physics*, 5th edition, John Wiley & Sons, Inc., New York, London, Sydney, Toronto, 1976.
13. D. E. Gray (contributing editor), *AIP Handbook*, 3rd edition, AIP, New York, 1972.
14. See sec. III of K. Odagiri and T. Yanagisawa, arXiv:1104.1247v1. This publication is currently under major revision.